Updating Structural Reliability Efficiently Using Load Measurement

N. De Koker[a,*], C. Viljoen[a], R. Lenner[a], S. W. Jacobsz[b]

[a] *Department of Civil Engineering, University of Stellenbosch, Stellenbosch, South Africa*

[b] *Department of Civil Engineering, University of Pretoria, Pretoria, South Africa*

[*] *Corresponding author email: ndekoker@sun.ac.za*

Abstract

The observation of an existing structure supporting a particular maximal load provides a direct constraint on the possible range of values its resistance capacity may take. The implied update of structural reliability allows monitoring and maintenance planning to be done from a risk optimal perspective. Existing proof load-based reliability updating techniques require multiple numerical computations which are often too cumbersome for routine use. By building on the assumptions of the first order reliability method, this study develops and validates a first order reliability updating approach which is computationally efficient. The resulting formulation is shown to be applicable to reliability problems tractably considered using the first order reliability method. This method is illustrated for two example structures: a reinforced concrete beam forming part of a highway bridge to which traffic loading data is applied, and a granular embankment forming a seawall on a shoreline mining operation for which the phreatic surface level is monitored.

Keywords: Updating Reliability; First-Order Reliability Method; Reliability of Existing Structures; Structural Health Monitoring

1. Introduction

Risk plays a principal role in the balance of safety and economy at the core of structural and geostructural engineering. Understood as the probability-weighted equivalent financial losses that would result from failure, it allows the aggregate effects of good design and maintenance practices to be expressed in financial terms that are useful in managing maintenance of infrastructure assets.

In the design of new structures, this balance is captured in an approximate sense by means of the target reliability embodied in the calibration of design standards [e.g. 1, 2, 3]. Existing structures are commonly assessed using these same techniques and standard calibrations, despite the fact that there is notable potential for reducing the uncertainty about performance limits through measurements of response to loading [4, 5] and comparison of these values to the design model predictions [6].

Knowledge of the change in reliability with time allows maintenance planning to be done from a risk optimal perspective [7], and is also of value when a structure is repurposed for a use in a different risk class [2, 4, 5].

The classification of uncertainty as epistemic versus aleatory [8, 9, 10], suggests a key perspective on time dependence in structural reliability problems. Loading parameters are predominantly aleatory and time varying, with uncertainty stemming from the inability to predict the future. Material parameters are mostly epistemic and spatially varying, with the possibility of reducing uncertainty by more representative sampling strategies.

To the extent that material deterioration can be accounted for, the lack of time-dependent variability in material parameters allows the lower bound on structural resistance capacity implied by its ability to resist a severe loading event observed in the past to be applied at the present time, albeit with a degree of uncertainty stemming from factors such as measurement error and the description of deterioration. Such a loading event can take the form of a controlled proof load test [e.g. 11, 12], or occur during the service life of the structure [e.g. 13, 14].

The first order reliability method (FORM) [15, 16] has been extensively applied to obtain reliability estimates for many common structural and geostructural design problems, and forms an integral part of standards calibration [1, 2]. The source of the utility and economy of the method is its simple geometrical formulation, by which it effectively reduces a many-dimensional integration problem to a one-dimensional standard normal probability determination.

Previous work on updating of structural reliability for existing structures using the lower bound on resistance capacity implied by severe loading or proof load-testing rely on a Bayesian updating formulation, in which the distribution of the structural resistance is truncated at the limit implied by the observed load [17, 18]. Updated reliability values are then obtained either by integration of the posterior distribution function [18, 19, 20, 21], or by updating the failure probability using the probability of the implied resistance bound conditional on the structure surviving the loading event [11, 22].

In the former approach, the irregular distribution shape due to truncation, coupled with the fact that typical structural and geostructural design problems involve resistance terms with multiple parameters with a variety of non-normal distribution

types, results in a strongly non-linear limit state function in standard normal space [17]. As a result, the updated reliability index cannot be directly determined using FORM, and instead needs to be obtained by numerical integration via a variant of the Monte-Carlo technique [e.g. 23]. Similarly, the latter approach requires evaluation of the conditional bound probability, again requiring Monte-Carlo integration.

This paper develops an efficient methodology for updating structural reliability following observations of severe loading. The method builds on the geometrical simplicity of FORM, reducing the multi-dimensional reliability updating problem to a two-dimensional combination of two related FORM solutions. The theoretical basis for this first order reliability updating method is developed in the following section, followed by validation and assessment of its performance for limit state functions with curvature at the design point. The method is then implemented for two example structures: firstly, a reinforced concrete beam forming part of a highway bridge with weigh-in-motion traffic loading measurements, and secondly a granular seawall embankment with piezometric records of the time variation in the phreatic surface.

2. Theoretical Development

2.1. Geometrical interpretation of reliability updating

Consider a simple performance function expressing the balance between the resistance capacity R and an applied load effect S. That is

$$g_1 = R - S, \tag{1}$$

for which the requirement that $g_1 \geq 0$ implies $R \geq S$. Load effect S is the result of a time-varying random process; R reflects a function of inherent properties of the structure and material, known only from a set of sample characterisations.

In a reliability context, $g_1 = 0$ represents a single limit state function delimiting the domain of parameter values associated with structural failure (Figure 1(a)), for which the probability is

$$p_f = \int_{g_1<0} f(R,S)dRdS = \int_{g_1<0} \phi_2(u_R,u_S)du_R du_S, \tag{2}$$

where u_X is the standard normal conjugate of random variable X, determined as $u_X = \Phi^{-1}(F(X))$, and ϕ_2 is the bivariate standard normal distribution function. Graphically, p_f corresponds to the integral of ϕ_2 over the area bounded by line ABC in Figure 1(a), and is associated with design point $\mathbf{u}_1^*$.

For any measured value $S = q_t$, the observation that the structure remains standing implies a lower bound on the associated range of values which R may take,

$$R_t \geq q_t, \tag{3}$$

with t denoting the fact that the observation is made at a specific time during the lifetime of the structure.

This inequality provides the essential basis for updating reliability based on the observation that the structure was able to resist a measured load. Defining a supplementary performance function

$$g_2 = R - q_t, \tag{4}$$

with associated design point $\mathbf{u}_2^*$, the updated probability of failure implied by this observation is then

$$\overline{p}_f = \int_{g_1<0 \cap g_2 \geq 0} \phi_2(u_R,u_S)du_R du_S, \tag{5}$$

that is, an integral over the area delimited by line ABD in Figure 1(a). Note that in the geometry of Figure 1 structural resistance R increases towards the origin on the u_R axis.

The updated reliability index is then

$$\overline{\beta} = \Phi^{-1}\left(1 - \overline{p}_f\right). \tag{6}$$

To avoid ambiguity due to the problem geometry, the reliability index is defined in terms of the failure probability, rather than the definition $\beta = \min\{\mathbf{u} \cdot \mathbf{u} \,|\, g_1 = 0\}$ [15, 16, 17].

For general problems in which the limit state function is non-linear, Equation 5 must be numerically integrated, normally using a Monte-Carlo technique. However, following a similar set of assumptions to that forming the basis of FORM, the two-dimensional geometry of the problem allows Equation 5 to be easily evaluated by numerical integration of ϕ_2 over the wedge ABD, which is described by the conditions

$$u_S \sin\theta_{12} + u_R \cos\theta_{12} > |\mathbf{u}_1^*| \quad \text{and} \quad u_R \leq |\mathbf{u}_2^*|, \tag{7}$$

where

$$\cos\theta_{12} = \frac{\mathbf{u}_1^* \cdot \mathbf{u}_2^*}{|\mathbf{u}_1^*||\mathbf{u}_2^*|}. \tag{8}$$

The updating method just described therefore makes the same assumption of limit state function linearity that underlie the first order reliability method (FORM).

2.2. Accounting for measurement error

Let ε be the independent random measurement error on q_t, so that g_2 becomes

$$g_2 = R - q_t - \varepsilon. \tag{9}$$

Limit state functions $g_1 = 0$ and $g_2 = 0$ now represent planes in the three-dimensional geometry shown in Figure 1(b), with design points $\mathbf{u}_1^*$ and $\mathbf{u}_{2|\varepsilon}^*$, respectively.

As shown in Figure 1(b) and (c), $\mathbf{u}_1^*$ and $\mathbf{u}_{2|\varepsilon}^*$ span a two-dimensional subspace which is orthogonal to both $g_1 = 0$ and $g_2 = 0$, with axial variables u_R' and u_S'. The geometry of this planar subspace is identical to that in Figure 1(a), so that the problem of determining $\overline{p}_f$ therefore reduces to that described in Equations 5-6, with design point vectors $\mathbf{u}_1^*$ and $\mathbf{u}_{2|\varepsilon}^*$. This is the geometrical essence of the first order updating methodology presented here.

2.3. Incorporating capacity decay

In the preceding discussion, the observation that q_{t_1} at time $t = t_1$ implied a corresponding lower bound R_{t_1} on the resistance capacity (Equation 3). However, if a period of time $\Delta t_{12} = t_2 - t_1$ has since elapsed to reach the present time t_2, the material may have weakened somewhat due to material decay (corrosion, alkali-silica reaction, fatigue, etc.), so that the lower bound R_{t_1} is no longer valid at t_2.

Let material decay be described by a model relation $\mathcal{L}(t)$ [11], such that

$$R(t) = R\mathcal{L}(t). \tag{10}$$

The performance functions describing the updated structural reliability at $t = t_1$ are then

$$g_1(t_1) = R\mathcal{L}(t_1) - S, \tag{11}$$

and

$$g_2(t_1) = R\mathcal{L}(t_1) - q_{t_1} - \varepsilon. \tag{12}$$

The effect of deterioration on $R(t_1)$ during Δt_{12} can be accounted for by expanding $R(t)$ about t_1. A first order estimate of $R(t_2)$ then follows as

$$R(t_2)' = R\mathcal{L}(t_1) + \Delta t_{12} R \frac{d\mathcal{L}(t)}{dt}\bigg|_{t_1}. \tag{13}$$

Noting from $g_2(t_1) = 0$ that $R\mathcal{L}(t_1) = q_{t_1} + \varepsilon$, the extrapolated supplementary performance function is then derived given by

$$g_2(t_2)' = R\mathcal{L}(t_2) - \Delta t_{12} R \frac{d\mathcal{L}(t)}{dt}\bigg|_{t_1} - q_{t_1} - \varepsilon, \tag{14}$$

which combined with $g_1(t_2)$ gives an extrapolated reliability update $\overline{\beta}'$ at time t_2. An observed value q_{t_2} at t_2 would be the new recorded maximum resisted load if $g_2(t_2)$ gives $\overline{\beta} \geq \overline{\beta}'$ (even if $q_{t_2} < q_{t_1}$).

2.4. Multi-dimensional problems

Equation 7 is general and applicable for design point vector pairs with any number of random variables ≥ 2, provided that the parameter space is Hermitian. Because it reduces the problem to a two-dimensional subspace spanned by $\mathbf{u}_1^*$ and $\mathbf{u}_{2|\varepsilon}^*$, the formulation is therefore general for multidimensional problems, provided that all aleatory random variables (i.e. non-boundable) are evaluated from measurements. Limits cannot be placed on individual material parameters, but the resistance term as a whole can be bounded. Note that this includes model uncertainty factors.

Parameter dependencies due to correlation are accounted for in the transformation to uncorrelated standard normal space [8], before the geometrical reduction to two dimensions is made. As a result, the method is general with respect to correlation among variables, provided that this is limited to pairs of aleatory or pairs of epistemic variables.

For a given generalised performance function

$$g(R_1, \ldots, R_n, S_1, \ldots, S_m), \tag{15}$$

in which the R_i denote the variety of possible parameters contributing to the structural resistance and S_i the set of loading parameters, the limit state functions corresponding to $\mathbf{u}_1^*$ and $\mathbf{u}_{2|\varepsilon}^*$ are then

$$\begin{aligned} &g_1(R_1, \ldots, R_n, S_1, \ldots, S_m, \varepsilon_1 = 0, \ldots, \varepsilon_m = 0) = 0, \quad \text{and} \\ &g_2(R_1, \ldots, R_n, S_1 = q_{1t}, \ldots, S_m = q_{mt}, \varepsilon_1, \ldots, \varepsilon_m) = 0, \end{aligned} \tag{16}$$

respectively .

3. Validation

Integration for the updated probability of failure via the linearised limit state function in Equation 7 is based directly on FORM, and assumes the limit state function ($g = 0$) to be linear in standard normal space. Although this is almost never truly the case for real structural problems, FORM remains tractable because the part of the parameter domain where the difference between $g = 0$ and its linear approximation at the design point becomes significant, fall predominantly in regions of very low probability density. The first order reliability updating formulation developed in Section 2 relies on a larger domain of the limit state function than that in the neighbourhood of the design point, and would therefore be somewhat more sensitive to curvature in $g = 0$.

To validate the formulation and explore the extent to which the method compares to the accuracy FORM, the first order reliability updating methodology is applied to a test performance function

$$g_u = \begin{cases} \cosh\left(\dfrac{\tilde{u}_S - \tilde{u}_R}{2}\sqrt{\kappa_d \beta_0}\right) - \dfrac{\tilde{u}_S + \tilde{u}_R}{2}, & \text{if } 0 \leq \kappa_d, \\ 2 - \cosh\left(\dfrac{\tilde{u}_R - \tilde{u}_S}{2}\sqrt{-\kappa_d \beta_0}\right) - \dfrac{\tilde{u}_S + \tilde{u}_R}{2}, & \text{if } -1/\beta_0 < \kappa_d < 0. \end{cases} \tag{17}$$

Here κ_d is the curvature at the design point $\mathbf{u}^* = (u_R^*, u_S^*)$, $\beta_0 = |\mathbf{u}^*|$, $\tilde{u}_R = u_R/u_R^*$, and $\tilde{u}_S = u_S/u_S^*$. Figure 2(a) illustrates $g_u = 0$ for a set of κ_d values. Note that for $\kappa_d = 0$, the limit state function reduces to the linear form assumed in FORM.

Hall [18] introduced a Bayesian approach in which the posterior distribution of the resistance, given observation $S = q_t \pm \varepsilon$, is given by

$$f_R'(r) = \frac{F_{\mathcal{N}}(r) f_R(r)}{\displaystyle\int_{-\infty}^{\infty} F_{\mathcal{N}}(r) f_R(r) dr}, \tag{18}$$

where $F_{\mathcal{N}}$ is the Gaussian cumulative distribution function with $\mu = q_t$ and $\sigma = \sigma_\varepsilon$, and f_R describes the distribution of resistance random variable R. As with Equation 2, and assuming R and S to be independent, the updated probability of failure is then

$$\overline{p}_f = \int_{g_u < 0} f_R'(r) f_S(s) dr ds, \tag{19}$$

from which the updated reliability follows.

The Bayesian approach does not assume linearity, and so gives the accurate updated p_f when curvature is present. However, the integration in Equation 19 becomes non-trivial when g is expensive to compute.

Figure 2(b) compares reliability indices determined using the first order updating method (Equation 7) to values determined using the Bayes equation (Equation 19), for the range of design point curvature values illustrated in Figure 2(a). Updating calculations used $\sigma_\varepsilon = 0.1\sigma_R$.

It can be seen that for a linear limit state function, the geometrical method yields identical results to the Bayesian approach of Hall [18]. That is, $\overline{\beta}_{\text{FORM}}/\overline{\beta} = 1.0$ for $\kappa_d = 0$.

Figure 2(b) also compares the dependence of FORM on limit state function curvature (labelled as "prior") with updated reliabilities determined using the first order approach. The latter show similar trends in curvature dependence to the prior reliabilities, although the magnitude of the resulting inaccuracy increases for q_t values away from the design point. As a general rule of thumb, geometrically updated reliability values will therefore be useful to the extent that the assumptions that underlie FORM are valid for a given problem.

4. Implementation for Example Structures

4.1. Weigh-in-motion traffic loading applied to reinforced concrete bridge

As a first example implementation, recorded weigh-in-motion data, in the form of point loads corresponding to the measured axle loads of individual vehicles, are applied to the moment influence line of a single supported beam. As simplification, it is assumed that the beam is supporting a single traffic lane and that a single vehicle governs the moment response. The data is obtained from the Roosboom measurement station in the left lane of the N3 toll route connecting Durban and Johannesburg [13], a primary route for freight transport from the Durban port to the economic centre of Gauteng.

Using computed moments for 721,000 vehicles measured in 356 days (2025 vehicles per day), and assuming the moments to be normally distributed [24, 25], synthetic data for 100 periods of 50 years was generated, from which daily and 50-year maxima subsets were selected. The resulting mean and variance of the daily maximum loading values was subsequently applied to generate a synthetic 50-year traffic loading time series as $365 \times 50 = 18{,}250$ Gumbel distributed random values. Parameters for the 50-year maxima were used in the reliability analysis (Table 1). The choice of Gumbel distribution is illustrative in this contribution; a detailed debate on the appropriate description to use for extreme traffic loading is beyond the scope of this study.

Material and loading parameters for the reinforced concrete beam under consideration are summarised in Table 1. For illustrative purposes, material decay is represented via an exponential decay model for the area of reinforcing steel with characteristic decay time τ, that is

$$\mathcal{L}(t) = \exp\left(-t/\tau\right). \tag{20}$$

The performance function for the primary reliability problem then follows its usual form,

$$g_1 = R_t - S_t \tag{21}$$

with [e.g. 26, 25]

$$R_t = \theta_R A_\text{s} f_\text{y} 0.9(h-c)\exp\left(-t/\tau\right), \quad \text{and} \tag{22}$$

$$S_t = \gamma_\text{c} whL^2/8 + Q, \tag{23}$$

where θ_R is the resistance model factor, A_s is the area of reinforcing steel, f_y its yield strength, Q is the imposed moment due to traffic, γ_c is the weight density of concrete, c is the cover depth, and h, w, and L is the depth, width, and length of the beam, respectively. A_s is adjusted to obtain $\beta_\text{ref} = 3.8$ (at $t = 0$), in accordance with Eurocode recommendations for 50 year reliability target values [1].

For a given measurement of the imposed moment, $Q = q_{t_1}$, made at time t_1, the observation constraint performance function at at time t_2 is then

$$g_2 = R_{t_2} + \frac{\Delta t_{12}}{\tau} R_{t_1} - S_{t_1} \tag{24}$$

with

$$R_{ti} = \theta_R A_\text{s} f_\text{y} 0.9(h-c)\exp\left(-t_i/\tau\right), \quad \text{and} \tag{25}$$

$$S_{t_1} = \gamma_\text{c} bhL^2/8 + q_{t_1} + \varepsilon. \tag{26}$$

Design points for g_1 and g_2 are computed at each locally maximal observation, for which the resulting updated reliability values are shown in Figure 3. Measurement error on q_t is estimated to be 5% [25]. Also shown is the updated reliability trace in which maintenance is performed after 30 years. In the absence of case-specific information, maintenance is assumed to return the reliability to the original target value and also to reset any evidence record of previously resisted loads.

Maximal observation events are seen to increase the structural reliability quite notably, with frequent updates in the reliability balanced by consistent deterioration of the structure. Figure 4 illustrates the reliability update effected by the spectrum of maximal observation values. In this example, the updated reliability is relatively sensitive to the uncertainty in the observation value (ε), reflecting relatively large α_ε values of 0.2 seen in the FORM analysis of g_2.

Following a similar methodology to that used in Section 3, accurate updated reliability values can be computed that do not make any assumptions regarding the shape of the limit state function. Comparison of updated reliability values computed using the Monte-Carlo method via Equation 5 to values computed using the first order reliability updating methodology, (Figure 5) show that for the reinforced concrete beam the first order method overestimates the updated reliability values by about 3%, consistent with the use of FORM in reliability analyses of concrete members.

4.2. Storm-induced surges in seawall embankment phreatic surface levels

The second implementation considers the stability of seawall embankments (landward slopes) at a mining operation along the southern African Atlantic coast. For the slope in question, excavation has progressed down to about 10 metres below the mean seawater level, protected by seawall embankments constructed

from locally excavated granular material that resist surging seawater levels during winter storms. In this illustrative example the geometries of the slope and the phreatic surface are simplified, and a circular slip surface is assumed (Figure 6).

The depth of the phreatic surface within the embankment is monitored using piezometric pressure transducers installed in boreholes. For this example, daily measurements of the phreatic surface height beneath the top shelf of the slope were used (Figure 6). The water level above the base of the slope ($L + L_0$) is fit with a lognormal distribution (Figure 7). The appropriate corresponding extreme value distribution for L in reliability analysis is therefore Type II [8], for which parameters were determined from the corresponding annual maxima via the same methodology followed in Section 4.1. Note that in this case daily values were assumed to have an autocorrelation time of one week, reflecting the influence of moon phases on the tides. Table 2 summarises the statistical parameters describing the data as well as the distribution parameters used in the reliability analysis. Because of the relatively short time period under consideration in this example, material decay is not considered.

The stability of the slope is assessed via the factor of safety $\mathcal{F}$, determined using Spencer's method [27, 28, 29], in which two unknowns ($\mathcal{F}$ and λ) are found by solving the equations (refer to Figure 6)

$$\sum_{\text{slices}} \zeta \left(\Delta x \sin\lambda - \Delta y \cos\lambda\right) = 0, \tag{27}$$

$$\sum_{\text{slices}} \zeta = 0, \tag{28}$$

with

$$\zeta = \frac{F_T \sin\alpha - c'\Delta d/\mathcal{F} - (F_T \cos\alpha - w\Delta d)\tan\phi'/\mathcal{F}}{\cos(\alpha-\lambda) + \sin(\alpha-\lambda)\tan\phi'/\mathcal{F}}. \tag{29}$$

Here, w is the pore water pressure (found from slice geometry and phreatic surface characterised via L), $F_T = W + F_V$, and Δx and Δy are moment arms at the base of each slice. The slope material is characterised by density γ, cohesion c', and friction angle ϕ'.

The primary performance function for reliability analysis is then

$$g_1 = \theta_{\mathcal{F}}\mathcal{F}(c', \phi', L, \varepsilon = 0) - 1, \tag{30}$$

from which the observation constraint performance function for a given observed value of $L = \ell_t$, follows as

$$g_2 = \theta_{\mathcal{F}}\mathcal{F}(c', \phi', L = \ell_t, \varepsilon) - 1, \tag{31}$$

with model uncertainty accounted for via $\theta_{\mathcal{F}}$ [30].

Parameter values are summarised in Table 2. Based on previous work [29], c' and ϕ' are the only material parameters considered with meaningful random variation. Imposed load atop the slope is not critical to the reliability analysis and is neglected here, so that the level of the phreatic surface (L) represents the time-dependent driver of failure uncertainty.

Design points for $g_1 = 0$ and $g_2 = 0$ are computed at each maximal phreatic surface level observation, for which the updated reliability values are shown in Figure 8. Figure 9 illustrates the reliability update effected by the range of maximal observation values. The updated reliability is relatively insensitive to the uncertainty in the observation value (ε), reflecting small α_ε values of only 0.02 seen in the FORM analysis of g_2. Comparison of the first order reliability update values to Monte-Carlo determinations via Equation 5 reveal (Figure 10) that for the limit-equilibrium analysis of slope stability, the first order method may underestimate the updated reliability values by 2-4%.

The acceptability of β values is generally judged within the context of the societal willingness to pay for increased safety [31]. The reference reliability value of $\beta_{\text{ref}} = 0.98$ for this slope is relatively low when compared to recommended values for civil structures [2, 3], but is comparable to estimates for slopes on active mines [32, 33]. Low β values for active mining slopes are considered acceptable provided that these structures are inaccessible to the public and are subject to continuous monitoring and maintenance [32].

5. Discussion

In general, accurate reliability update values would require numerical integration of Equation 5 or Equation 19. Direct numerical integration [17, 18, 20] becomes prohibitive for multidimensional problems, so that such evaluations generally require the use of Monte-Carlo techniques [19, 34, 35], which still represent a significant undertaking when numerical simulations are required to evaluate the performance function. Similarly, Bayesian updating of the probability of failure [11, 22] require the probability of the observed load conditional on failure not occurring to be evaluated, again involving repeated evaluation of the performance function.

Because the first order updating method relies on a linear limit state function, it can be readily used to extend reliability analyses of structural and geostructural problems usually analysed using FORM. This includes the common failure modes associated with structural members [e.g. 8, 36], as well as commonly encountered geostructures [e.g. 29, 37, 38].

The analyses performed in the present study assume that a single failure mode dominates. In cases where multiple failure modes are present, the probability of failure reflects the union of all these modes. The reliability index reflects failure of a given structural entity, without specific reference to the mode of failure. Observing a particular load implies bounds on a subset of material properties via a given failure mode, properties that also contribute to the resistance of another mode [18]. However, using this information to update reliability requires all the relevant failure modes to be taken into account. Such a scenario would require multiple $g_1 = 0$ surfaces to be defined, and is beyond the scope of the first order method presented.

The two example implementations in Section 4 illustrate the effect of measured structural performance on the reliability of existing structures. An observation in which the structure resists a relatively large (though not unrealistic) load, eliminates

a section of parameter space from the possible parameter combinations that can result in failure, and shifts the reliability upwards by a notable amount. A larger number of smaller load measurements contribute to the updated reliability trace as the characteristic deterioration time decreases, as well as following maintenance, in which the lower bound history on resistance capacity is reset.

The material decay model assumed in Section 4.1 is purposely generic for illustration purposes; other simple forms have been used in previous work [11]. More realistic descriptions of material deterioration would be tailored to a specific set of mechanisms, for example for alkali-silica reaction in concrete, fatigue in steel, or internal particle erosion in embankments. Any of these mechanisms would by necessity involve a number of additional parameters treated as random variables; the formalism is general and can be applied in these cases provided that the time derivative of the resistance term (Equation 14) exists and can be evaluated.

Practical implementation of the method for real structures must be done in the context of loads that the structure is known to have been subjected to. Observations of such loading can take the form of semi-continuous monitoring, as is the case in the two examples discussed, or of controlled load tests.

As such, the observation that, despite deterioration of the structure, reliability is sustained at higher values than the reference value of the original target reliability, should not be interpreted as implying that maintenance is unnecessary. Any updated reliability value carries the assumption that no failure (or damage) occurred during the associated loading event, and the lower reliability value prior to the update reflects the fact that the probability of failure during severe loading is not negligible.

6. Conclusions

The observation of an existing structure supporting a particular maximal load provides a direct constraint on the possible range of values its resistance capacity may take. The implied update of the structural reliability allows monitoring and maintenance planning to be done from a risk optimal perspective. Proof load-based reliability updating techniques require multiple numerical computations which are often too cumbersome for routine use.

By building on the assumptions of the first order reliability method, a computationally efficient first order reliability updating approach is developed and validated. The formulation is shown to be applicable to any reliability problem tractably considered using the first order reliability method.

Implementation for example structures using characteristic loading histories illustrates the effect of measurements on the uncertainty in resistance capacity. Updated reliability traces associated with these time histories indicate that decreases in the probability of failure of two to three orders of magnitude can be obtained by incorporating realistic maximal loading observations into reliability estimates for existing structures.

It is hoped that the technique can aid in planning optimal infrastructure maintenance and monitoring programmes, as well as calibration of partial factor-based standards for existing structures. In the framework of this objective, a number of questions should be considered in further work. Notable among these are: the combination of loading and health monitoring data into a single updating framework, including more detailed material-specific deterioration models, generalising to problems with multiple failure modes, and exploring how observation information can be transferred across maintenance intervention events.

Acknowledgements

Reliability analysis computations for the two example structures were performed using the UQLab reliability analysis library [39]. Colin Caprani and two anonymous reviewers provided valuable input towards improving the manuscript.

7. References

[1] H. Gulvanessian, Eurocode: Basis of structural design, in: J. Roberts (Ed.), The essential guide to Eurocodes transition, British Standards Institution, London, 2010.

[2] JCSS, Risk Assessment in Engineering: Principles, System Representation & Risk Criteria, Joint Committee on Structural Safety, available at http://www.jcss.ethz.ch/, 2008.

[3] ISO 2394:2014, General principles on reliability for structures, International Organization for Standardization, Geneva, 2014.

[4] R. Caspeele, R. Steenbergen, M. Sýkora, Partial factor methods for existing concrete structures, vol. 80, Fédération internationale du béton (fib), 2016.

[5] D. Hosser, C. Klinzmann, R. Schnetgöke, A framework for reliability-based system assessment based on structural health monitoring, Structure and Infrastructure Engineering 4 (4) (2008) 271–285.

[6] F. N. Catbas, M. Susoy, D. M. Frangopol, Structural health monitoring and reliability estimation: Long span truss bridge application with environmental monitoring data, Engineering Structures 30 (9) (2008) 2347–2359.

[7] B. R. Ellingwood, Risk-informed condition assessment of civil infrastructure: state of practice and research issues, Structure and Infrastructure Engineering 1 (1) (2005) 7–18.

[8] A. H. Ang, W. H. Tang, Probability Concepts in Engineering Planning and Design: Volume II Decision, Risk, and Reliability, John Wiley and Sons, New York, 1st edn., 1984.

[9] M. H. Faber, On the treatment of uncertainties and probabilities in engineering decision analysis, Journal of Offshore Mechanics and Arctic Engineering 127 (3) (2005) 243–248.

[10] A. Der Kiureghian, O. Ditlevsen, Aleatory or epistemic? Does it matter?, Structural Safety 31 (2008) 105–112.

[11] M. H. Faber, D. Val, M. Stewart, Proof load testing for bridge assessment and upgrading, Engineering Structures 22 (2000) 1677–1689.

[12] E. Lantsoght, Y. Yang, R. Tersteeg, C. Veen, A. De Boer, Development of Stop Criteria for Proof Loading, 1064–1071, 2016.

[13] R. Lenner, D. de Wet, C. Viljoen, Traffic characteristics and bridge loading in South Africa, Journal of the South African Institution of Civil Engineering 59 (4) (2017) 34–46.

[14] J. Botha, J. Retief, C. Viljoen, Uncertainties in the South African wind load design formulation, Journal of the South African Institution of Civil Engineering 60 (3) (2018) 16–29.

[15] A. M. Hasofer, N. C. Lind, Exact and invariant second-moment code format, Journal of the Engineering Mechanics Division, ASCE 100 (1974) 111–121.

[16] R. Rackwitz, B. Fiessler, Structural reliability under combined random load sequences, Computers and Structures 9 (1978) 484–494.

[17] T. Lin, A. Nowak, Proof Loading and Structural Reliability, Reliability Engineering 8 (1984) 85–100.

[18] W. Hall, Reliability of Service-Proven Structures, Journal of Structural Engineering 114 (1988) 608–624.
[19] D. Straub, Reliability updating with equality information, Probabilistic Engineering Mechanics 26 (2) (2011) 254–258.
[20] C. Caprani, J. Padgett, W. Chiu, Strategies for safety assurance of bridges exposed to multiple climate-related threats, ISBN 978-1-138-00103-9, 769–777, doi:10.1201/b17063-112, 2014.
[21] M. Kapoor, J. Schmidt, J. Sørensen, S. Thöns, A decision theoretic approach towards planning of proof load tests, in: 13th International Conference on Applications of Statistics and Probability in Civil Engineering, 1064–1071, 2019.
[22] H. Brüske, S. Thöns, Value of preconstruction proof loading information for structural design, Wind Energy In Press, doi: https://doi.org/10.1002/we.2398.
[23] S.-K. Au, J. L. Beck, Estimation of small failure probabilities in high dimensions by subset simulation, Probabilistic engineering mechanics 16 (4) (2001) 263–277.
[24] J. Bogath, K. Bergmeister, Neues lastmodell für Straßenbrücken, Bauingenieur 74 (6).
[25] R. Lenner, M. Sýkora, Partial factors for loads due to special vehicles on road bridges, Engineering Structures 106 (2016) 137–146.
[26] M. Sýkora, M. Holický, J. Marková, Verification of existing reinforced concrete bridges using the semi-probabilistic approach, Engineering Structures 56 (2013) 1419–1426.
[27] E. Spencer, A Method of analysis of the Stability of Embankments Assuming Parallel Inter-Slice Forces, Géotechnique 17 (1) (1967) 11–26.
[28] J. M. Duncan, S. G. Wright, Soil Strength and Slope Stability, John Wiley and Sons, New York, 2nd edn., 2005.
[29] N. De Koker, P. W. Day, A. Zwiers, Assessment of Reliability Based Design of Stable Slopes, Canadian Geotechnical Journal 56 (2019) 495–504, doi:10.1139/cgj-2018-0149.
[30] M. Dithinde, K. K. Phoon, J. Ching, L. Zhang, J. Retief, Statistical characterisation of model uncertainty, in: K. K. Phoon, J. V. Retief (Eds.), Reliability of Geotechnical Structures in ISO2394, CRC Press, London, UK,, 127–154, 2016.
[31] K. Fischer, C. Viljoen, J. Köhler, M. H. Faber, Optimal and acceptable reliabilities for structural design, Structural Safety 76 (2019) 149–4161.
[32] H. A. D. Kirsten, Significance of the probability of failure in slope engineering, The Civil Engineer in South Africa 25 (1983) 17–23.
[33] F. Silva, T. W. Lambe, W. A. Marr, Probability and risk of slope failure, Journal of Geotechnical and Geoenvironmental Engineering 134 (12) (2008) 1691–1699.
[34] I. Papaioannou, D. Straub, Reliability updating in geotechnical engineering including spatial variability of soil, Computers and Geotechnics 42 (2012) 44–51.
[35] S. Jiang, I. Papaioannou, D. Straub, Bayesian updating of slope reliability in spatially variable soils with in-situ measurements, Engineering Geology 239 (2018) 310–320.
[36] R. Melchers, Structural Reliability Analysis and Prediction, John Wiley & Sons, New York, 1999.
[37] B. K. Low, K. K. Phoon, Reliability-based design and its complementary role to Eurocode 7 design approach, Computers and Geotechnics 65 (2015) 30–44.
[38] N. De Koker, P. W. Day, Assessment of reliability-based design for a spectrum of geotechnical design problems, Proceedings of the Institution of Civil Engineers - Geotechnical Engineering 171 (2) (2018) 147–159, doi:10.1680/jgeen.17.00047.
[39] S. Marelli, B. Sudret, UQLab: A Framework for Uncertainty Quantification in Matlab, in: Vulnerability, Uncertainty, and Risk, American Society of Civil Engineers, Reston, VA, ISBN 9780784413609, 2554–2563, doi: 10.1061/9780784413609.257, 2014.
[40] T. T. E. Kanime, Reliability analysis of seawalls facilitating coastal mining, Masters Thesis: Stellenbosch University, 2018.

Table 1: Parameters used in reliability analysis and updating of the reinforced concrete beam in Section 4.1.

Measurements		μ	σ	
M_Q(daily)	Gumbel	653	33.9	kNm
ε	Normal[a]	0	43.2	kNm
Actions		μ	σ	
M_Q(annual)	Gumbel	864	21.6	kNm
Resistance Parameters		μ	σ	
θ_R	Lognormal[b]	1.1	0.11	
A_s	-	6.45×10^{-3}		m^2
f_y	Lognormal[b]	500	25	MPa
h	Normal[b]	1.0	0.02	m
c	Gamma[b]	50	1.5	mm
L	-	10		m
γ_c	-	25		kN/m^3

a – [25], b – [26]

Table 2: Parameters used in reliability analysis and updating of the seawall slope in Section 4.2. Limit equilibrium calculations used 50 slices for the slip section. Mean parameter values yield factor of safety $\mathcal{F} = 1.17$.

Measurements		μ	σ	
L(daily)	Lognormal	3.01	0.92	m
ε	Normal	0	0.2[a]	m
Actions		λ_1	λ_2	
L(annual)	Type II	5.75	0.83	m
Resistance Parameters		μ	σ	
$\theta_{\mathcal{F}}$	Lognormal[b]	1.19	0.32	
ϕ'	Lognormal[c]	33[d]	3.3	degrees
c'	Lognormal[c]	2.0[d]	0.8	kPa
γ	-	17.3[d]		kN/m^3
B	-	35[d]		m
H	-	20[d]		m
L_0	-	4.7		m

a – estimate of borehole depth accuracy, b – [30], c – [29], d – [40]

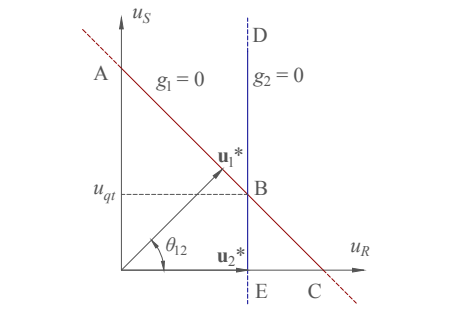

(a)

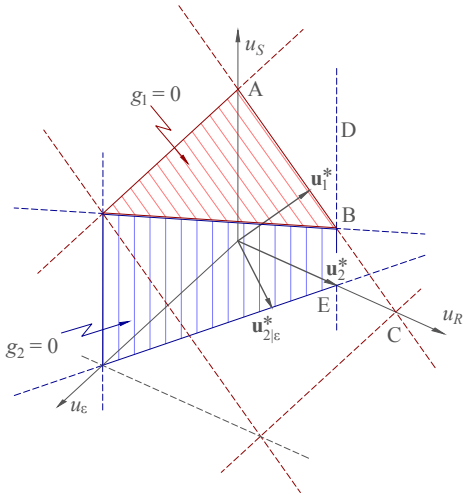

(b)

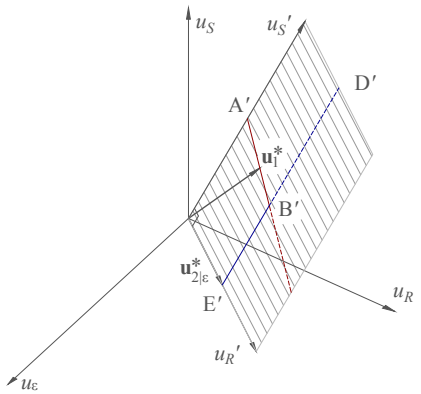

(c)

Figure 1: Geometrical basis for the first order reliability updating formulation.

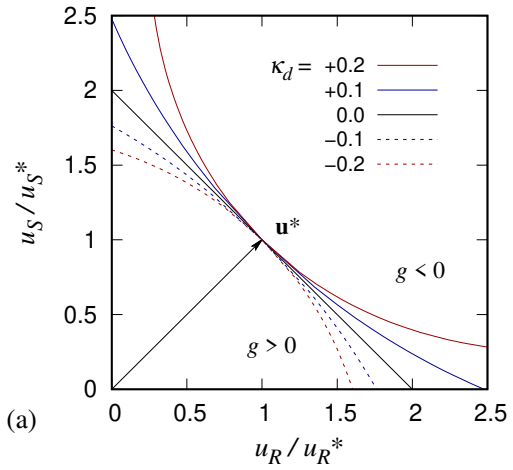

(a)

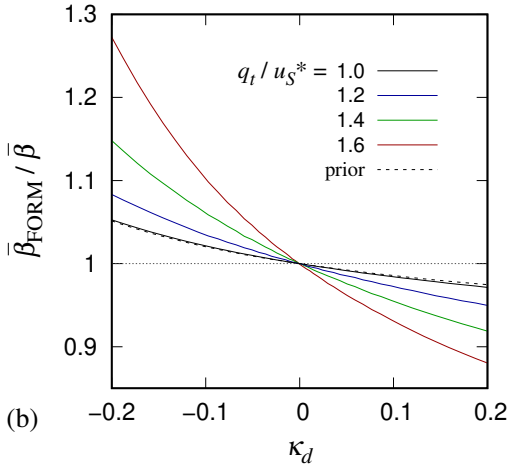

(b)

Figure 2: Validation of first order reliability updating method for limit state function with curvature at the design point. All calculations use $\sigma_\varepsilon = 0.1\sigma_R$

.

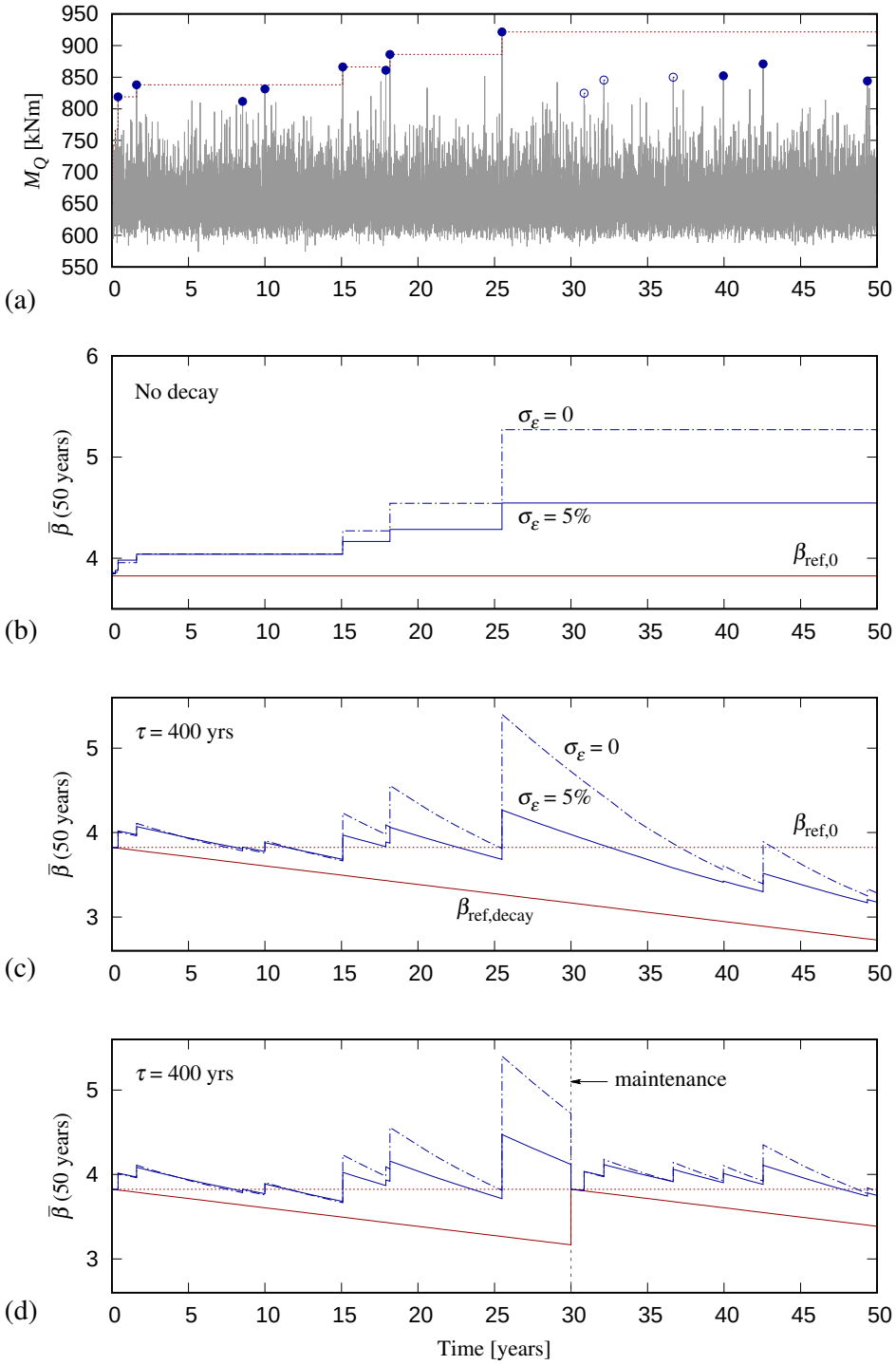

Figure 3: Updated reliability variation with time for the reinforced concrete beam, based on the synthetic data trace of daily maxima in (a). Open and closed symbols reflect observations used in updating with (d) and without (c) maintenance, respectively.

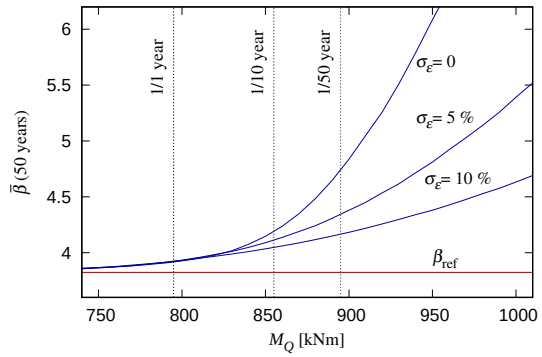

Figure 4: Updated reliability values that the range of extreme traffic loading values would yield for the reinforced concrete beam, from $\beta_{\text{ref}} = 3.8$. Exceedence probabilities are indicated via observational return periods.

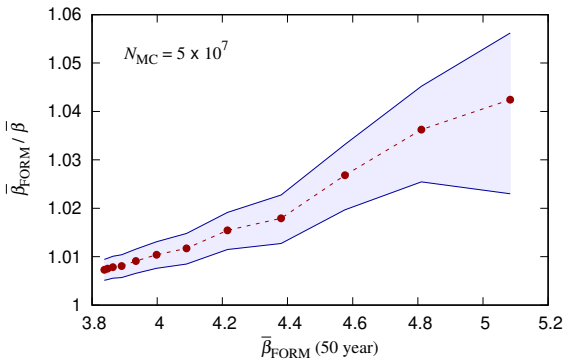

Figure 5: Ratio of FORM-based updated β and values determined using Monte-Carlo integration over the full non-linear limit state functions, determined for the reinforced concrete beam for a series of progressively more severe loading events. Shaded area denotes a 95% confidence interval on Monte-Carlo computations.

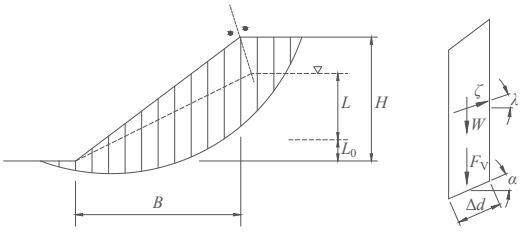

Figure 6: Cross section schematic of the slope geometry and slice parameters used in Section 4.2.

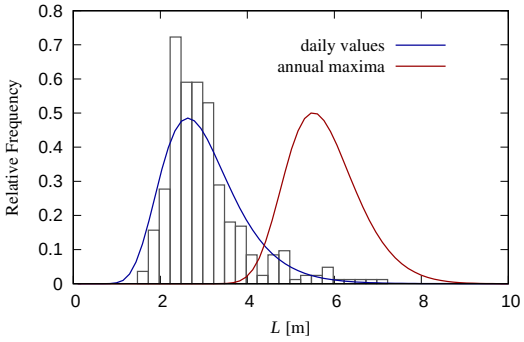

Figure 7: Frequency distribution of daily water level measurements, represented via a log-normal distribution, for which annual maximum values are Type II distributed.

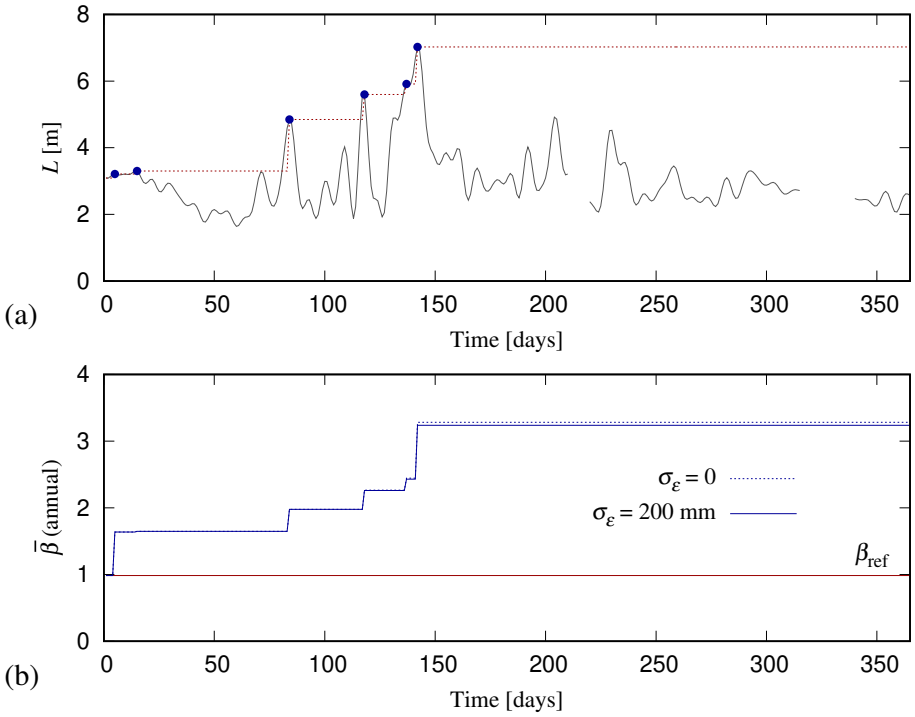

Figure 8: Updated slope reliability with time for the seawall slope over a period of a year, based on maxima in the measured water level time history.

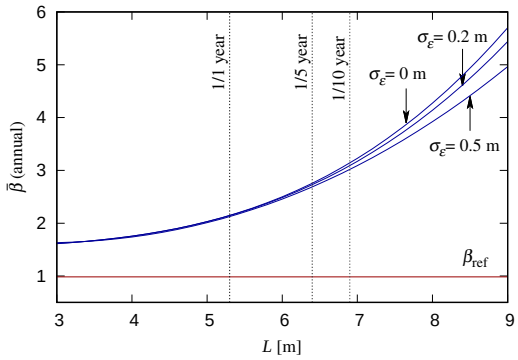

Figure 9: Updated reliability values that the range of extreme phreatic surface level values would yield for the seawall slope, from $\beta_{\text{ref}} = 0.98$. Exceedence probabilities are indicated via observational return periods.

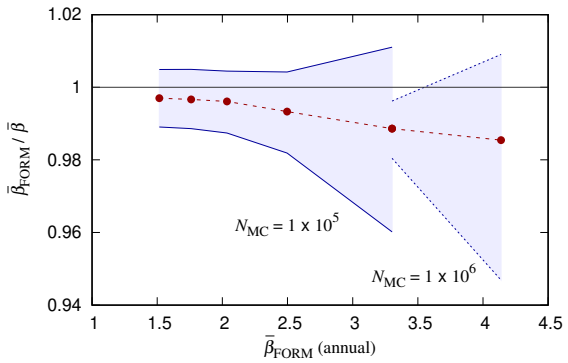

Figure 10: Ratio of FORM-based updated β and values determined using Monte-Carlo integration over the full non-linear limit state functions, determined for the seawall slope for a series of progressively more severe loading events. Shaded area denotes a 95% confidence interval on Monte-Carlo computations.